Specific heat of normal liquid ^{3}He

Dennis S. Greywall
Bell Laboratories, Murray Hill, New Jersey 07974
(Received 22 October 1982)

High-precision, constant-volume specific-heat measurements were made on pure liquid ^{3}He in the normal phase. The data were obtained for temperatures between 7 mK and 2.5 K and in the pressure range 0—32.5 bar. Below 30 mK the results are about 25% *greater* than those from two other very recent experiments and about 10% *less* than the earliest values. Between 30 and 500 mK the data agree with all previous measurements to within about ±5%. Above 500 mK the present measurements are the first to be reported at other than saturated vapor pressure. Several checks indicate that only the present very-low-temperature data are thermodynamically consistent. Consequently, adjustments must be made in all of the previously determined Landau parameters. In agreement with theory, the low-temperature specific-heat data at all densities can be described well by a function which includes terms only in T and in $T^3\ln T$. This form, however, seems to apply out to higher temperatures than expected. From the coefficient of the $T^3\ln T$ term values of the Landau parameter F_1^a are extracted which are consistent with other determinations.

I. INTRODUCTION

In two very recent experiments[1,2] the specific heat of liquid ^{3}He was measured in a temperature range extending below 1 mK and over the entire pressure range of the liquid phase. The primary goal of these studies was to provide information concerning the deviations from the Bardeen-Cooper-Schreiffer (BCS) theory as applied to superfluid ^{3}He. Even though the findings from these two experiments are in excellent agreement, serious questions arise because the normal-phase data differ appreciably from previous measurements.[3–7] The discrepancy, which in the worst case is 40%, is particularly significant since it is from the low-temperature normal-phase specific-heat results that one extracts the effective mass of the ^{3}He quasiparticles. This parameter plays a very fundamental role, not only in the Landau theory of the normal liquid, but also in the various theories which apply to superfluid ^{3}He. Unfortunately, because of experimental limitations, the newest[1,2] sets of data extend up in temperature only to about 10 mK, and consequently the important direct comparison with many of the older higher-temperature experiments[8–10] is not possible. Between roughly 30 and 500 mK all of the previous specific-heat measurements agree to within about 10%.

In this paper new high-precision C_V results are reported for the normal phase of liquid ^{3}He. The data span the temperature range 7 mK to 2.5 K and the pressure range 0 to 32.5 bar. At the lowest temperatures the present data lie in between the two extremes but closer to the older values[3–7] and at intermediate temperature approximately in the middle of the smaller spread of previous results.[4–10] Above 0.5 K the present data are the first to be reported at other than saturated vapor pressure (SVP).[11,12] Although there is no obvious explanation for the very large spread of previous results at low temperature, several checks performed on the data indicate that only the present specific-heat measurements are thermodynamically consistent. A brief report on a portion of this work has previously been published.[13]

II. EXPERIMENTAL DETAILS

A. Calorimeter

A cross-sectional drawing of the calorimeter is shown in Fig. 1 and some of the physical parameters are summarized in Table I. The heavy-walled sample cell was machined from high-purity silver and had a nominal volume of 11 cm^3. Epoxy[14] was used to form the seal at the point where the cylindrical body threaded into the base. Nineteen silver rods (1.3-mm diameter, 5 cm long) were welded into holes which were drilled through the base in a close-packed pattern with a center-to-center spacing of 3.5 mm. Silver powder was sintered around each of these rods using a graphite mold to form 2.8-mm-diameter posts. The silver powder[15] used

 ©1983 The American Physical Society

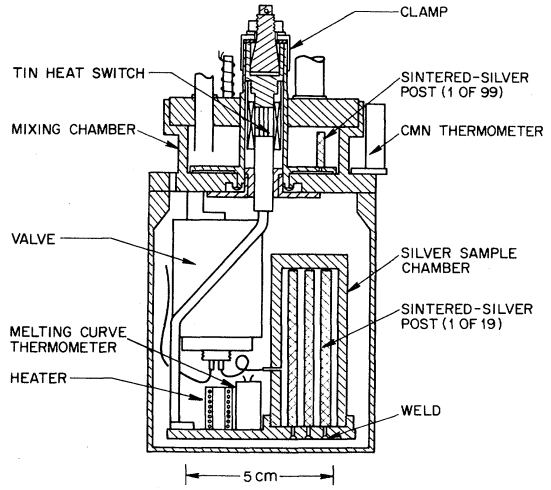

FIG. 1. Calorimeter.

(flakes with a diameter of $\lesssim 3\ \mu$m and a thickness of $\sim 0.2\ \mu$m) had a magnetic impurity level of about 2 ppm.[16] From Brunaver-Emmett-Teller (BET) adsorption measurements using krytpon the total surface area was determined to be $\sim 2\ m^2$. This relatively small surface area was sufficient to reduce the thermal time constant to a manageable level at low temperatures, but still small enough to ensure that any surface contribution[1] to the ^{3}He heat capacity would be completely negligible. Because the silver posts penetrated the entire sample chamber none of the ^{3}He sample was more than ~ 1 mm from the nearly isothermal silver surface. This meant that the internal time constant of the ^{3}He did not become larger than about 30 sec.

We comment that one reason for choosing not to make the cell from copper was that many,[17,18] if not all, types of copper exhibit an anomalous T^{-2} contribution to the heat capacity. Had the cell been constructed of copper this anomalous contribution would have corresponded to roughly 5% of the sample heat capacity at 7 mK. The results of Haavasoja *et al.*,[1] and also the present work, indicate that if this anomaly exists for silver as well, it must be at least an order of magnitude smaller.

TABLE I. Calorimeter details.

Sample volume:	$11.43 \pm 0.03\ cm^3$
Volume of silver sinter:	$3.5\ cm^3$
Surface area of sinter:	$2\ m^2$
Principal construction materials:	
Silver:	278.3 g
Silver sinter:	14.5 g
Copper:	9.2 g
Be-Cu:	3.4 g
Cu-Ni:	0.2 g
Pt-W:	0.2 g
1266 epoxy:	0.2 g
Speer resistor:	0.2 g

The cell was mechanically supported below the mixing chamber of a dilution refrigerator with two 6.4-mm-diameter graphite rods. For the data obtained below 0.5 K, thermal connection between the mixing chamber and cell was via a 3.2-mm-diameter silver rod in series with a tin heat switch. The tin was in the form of 19 0.5-mm-diameter, high-purity wires which were about 1 cm long; they were soldered with tin. Graphite pieces were used to give the switch mechanical strength. A clamp which employed a conical wedge was used to attach the cold end of the switch to the mixing chamber. The silver rod was attached to the cell using a silver foot welded to the end of the rod and a silver 4-40 screw. All mating surfaces were gold plated. For the data obtained above 0.5 K, the heat-switch assembly was replaced by a 10-cm length of 0.1-mm-diameter copper wire.

A melting-curve thermometer, a Speer carbon thermometer (470 Ω), a previously calibrated germanium thermometer, and two nearly identical 10-k Ω wire resistors were also attached to the base of the cell. The carbon resistor was compared with one of the 10-k Ω resistors in an ac bridge circuit. The second resistor was the calorimeter heater.

The wire resistors were made by noninductively winding a 7.6-m length of 0.025-mm-diameter Pt-W wire around a silver post. The resistors were varnished to the post, and had NbTi superconductor leads. Pt-W (0.92, 0.08) (Ref. 19) wire has a T^{-2} contribution to its heat capacity ($CT^2 \approx 10^{-5}$ mJ/g) which is negligibly small compared to the ^{3}He heat capacity. The resistance of this wire decreases by about 7% between room temperature and 77 K and by another 0.7% between 77 and 4 K. Below 4 K the resistance increases at a rate of about 0.015% /K. So even though the heater-wire temperature does rise significantly above the sample temperature during the application of a heat pulse, the resistance of the wire does not vary appreciably. Note that had the heater wire been simply suspended in the ^{3}He sample the change in wire temperature would have been an order of magnitude larger due to the larger boundary resistance. For our heater and typical power-dissipation rates we estimate the temperature rise to have been less than 1 K at 10 mK and smaller at higher temperatures. No correction was applied for any temperature dependence of the heater resistance. A silver shield surrounded the heater (Fig. 1) to guard against heat being lost by radiation.

Two short lengths of 0.40-mm i.d. copper tubing

were epoxied into close-fitting holes drilled into the cylindrical wall of the cell. One was used to evacuate the sample chamber prior to the cool down of the apparatus. It was crimped and soldered closed after pumping. A copper-nickel filling capillary (0.10-mm i.d., 0.30-mm o.d. by 15-cm long) was soldered into the second copper tube. The fine capillary led directly to a hydraulically operated ^{4}He valve[20] also mounted on the mixing chamber. Locating the valve at low temperature ensured that the number of moles of sample did not change as a function of temperature due to the contraction or expansion of the sample or as a function of time due to the change in ^{4}He-bath level. The heat-capacity measurements thus accurately correspond to C_V. A cerium magnesium nitrate (with grease) thermometer[21] and a heater mounted on the mixing-chamber platform were used to control its temperature so that some adjustment could be made on the warming and cooling drift rates of the cell.

B. Thermometry

Two different thermometers were used to measure the cell temperature over the range 7 mK to 2.5 K. Above 150 mK we used a 470-Ω Speer carbon resistor. At lower temperatures we used a ^{3}He–melting-curve thermometer which is described in detail in Ref. 21. The melting-curve thermometer was used at low temperature because of its high sensitivity and fast thermal response. Moreover, having the ^{3}He heat-capacity data directly related to a specific calibration of the melting curve means that the results can be unambiguously adjusted for any subsequent modifications in the P-T relation.

The capacitance of the melting-curve thermometer was measured using a ratio transformer bridge circuit and a reference capacitor kept in a liquid-nitrogen bath. The reference had a long-term stability of a few ppm with the oscillations following changes in the barometric pressure. The pressure calibration of the gauge was performed near 1 K and in the range $27 < P < 35$ bar using a dead-weight tester. A uniform shift of 2 mbar was then applied to force the measured pressure at the minimum in the melting curve to coincide with the calibration[21] value, namely 29.316 bar. Each time the calorimeter was warmed above the melting-curve minimum temperature (0.318 K) a determination of $P_{\min}$ was made to be sure that there were no shifts in the pressure calibration. The bridge was operated at 1 kHz and with an excitation of 2 V rms. At this drive level no heating could be detected.

The resistance of the carbon thermometer varnished to the base of the cell was also measured using a ratio transformer bridge circuit. The reference was a 10-KΩ Pt-W wire resistor (see Sec. II A) mounted on the base plate. This bridge was driven at 31 Hz and at levels of 0.8 mV below 0.5 K and 3 mV above 0.5 K. With these excitations there was a small amount of self-heating in the thermometer. However, because of the high-amplitude stability of the drive signal this did not introduce any difficulties. The calibration of this thermometer was performed during the course of data taking and repeated for each ^{3}He sample. Comparison was made with a calibrated germanium thermometer also mounted on the base of the cell. This latter thermometer had been calibrated previously[21] using the ^{3}He vapor-pressure scale[22] corrected to T_{76} (Ref. 23) for $T > 0.3$ K. For $T < 0.3$ K, a National Bureau of Standards (NBS) superconducting fixed-point device and a CMN thermometer[21] determined the temperature. A comparison of temperatures determined using the present melting-curve thermometer and the germanium resistor agreed to better than 0.1 mK for $T > 100$ mK. Each set of calibration data for the carbon resistor was fitted using the expression[24]

$$T^{1/4} = \sum_{i=0}^{n} a_i [\ln(R - 1250)]^i . \tag{1}$$

The rms deviations of the temperature readings were about 0.03% for fits with $n = 3$ and $100 < T < 600$ mK, and about 0.04% for $n = 5$ and $0.4 < T < 2.6$ K.

C. Melting curve calibration

In Ref. 21 a calibration of the ^{3}He melting curve was presented which was based on new P-T measurements between 7 and 330 mK and on the data of Halperin *et al.*[3] below 22 mK. The temperatures for the new data were determined using a CMN thermometer with the Δ [$\chi \propto (T - \Delta)^{-1}$] being chosen so as to cause the P-T data to agree with the Halperin *et al.* results in the region of overlap. The uncertainty in this melting-curve scale is then related to the accuracy of the Halperin *et al.* data which hinges most directly on their determination of the superfluid transition temperature. Errors can also arise, however, from differences in the pressure scales used. The accuracy of the $P - P_{\min}$ determinations are probably of the order of 3 mbar (out of 5000 mbar) at low temperature in both experiments. Moreover, Halperin *et al.* used a ^{3}He sample with 200 ppm ^{4}He which means that their minimum was depressed by about 2 mbar. Consequently, it is estimated that the overall accuracy of the melting-curve calibration of Ref. 21 is roughly 0.3 mK at low temperature, if pressures are measured relative to $P_{\min}$.

Having made ^{3}He specific-heat measurements using our melting-curve thermometer allows us now to reanalyze our melting-curve calibration data without having to rely on the data of Halperin *et al.* This is possible if we assume that C_V/RT tends toward a constant value at very low temperature as predicted by the Landau Fermi-liquid theory. (R is the gas constant.) In Fig. 2 we have plotted C_V/RT at $P=0$ determined using melting-curve calibrations based on different values of the CMN Δ. We conclude that Δ is equal to 0.40 ± 0.05 mK for our particular CMN thermometer. The temperature scale determined in this manner differs from that used in Ref. 21 by about 0.25 mK at low temperatures. This change is within the estimated uncertainty in that scale which was discussed above.

The ^{3}He melting-curve calibration based on $\Delta=0.40$ mK is described well by the relation

$$P-P_{\min}=\sum_{i=-2}^{5} a_i T^i , \tag{2}$$

with

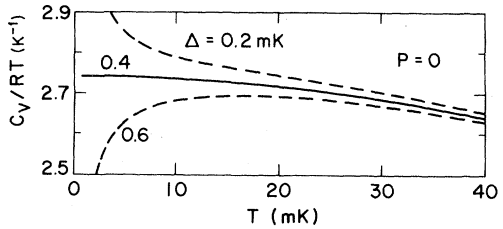

FIG. 2. C_V/RT for ^{3}He at $P=0$. The three curves are based on melting-curve calibrations determined using various values of the CMN Δ.

$$a_{-2}=2.1895\times10^{-8},\quad a_{-1}=-8.1989\times10^{-5},$$

$$a_0=5.162\,54,\quad a_1=-44.0395,$$

$$a_2=153.846,\quad a_3=-350.634,$$

$$a_4=594.115,\quad a_5=-465.947.$$

Several values determined using Eq. (2) are listed in Table II. The relative temperature deviations from the calibration of Ref. 21 are plotted in Fig. 3. Between T_A and 22 mK, Eq. (2) also describes the re-

TABLE II. ^{3}He–melting-curve parameters determined using Eq. (2).

T (mK)	$P-P_{\min}$ (bar)	dP/dT (bar K^{-1})	T (mK)	$P-P_{\min}$ (bar)	dP/dT (bar K^{-1})
3	5.0069	−35.6	90	2.2248	−23.3
4	4.9697	−38.4	95	2.1105	−22.4
5	4.9306	−39.6	100	2.0004	−21.6
6	4.8907	−40.2	110	1.7918	−20.1
7	4.8504	−40.4	120	1.5982	−18.6
8	4.8100	−40.4	130	1.4188	−17.3
9	4.7696	−40.4	140	1.2528	−15.9
10	4.7292	−40.3	150	1.0996	−14.7
11	4.6890	−40.1	160	0.9585	−13.5
12	4.6489	−40.0	170	0.8289	−12.4
14	4.5695	−39.5	180	0.7103	−11.3
16	4.4909	−39.1	190	0.6023	−10.3
18	4.4132	−38.6	200	0.5045	−9.3
20	4.3365	−38.1	210	0.4164	−8.3
25	4.1492	−36.8	220	0.3377	−7.4
30	3.9681	−35.6	230	0.2681	−6.5
35	3.7931	−34.4	240	0.2072	−5.7
40	3.6241	−33.2	250	0.1548	−4.8
45	3.4609	−32.1	260	0.1106	−4.0
50	3.3033	−31.0	270	0.0742	−3.3
55	3.1511	−29.9	280	0.0454	−2.5
60	3.0043	−28.9	290	0.0240	−1.8
65	2.8625	−27.9	300	0.0095	−1.1
70	2.7257	−26.9	310	0.0017	−0.5
75	2.5936	−25.9	320	0.0002	0.2
80	2.4663	−25.0	330	0.0046	0.7
85	2.3434	−24.1			

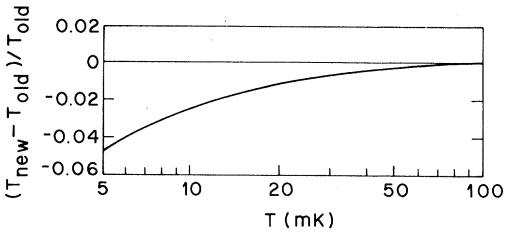

FIG. 3. Difference between our new [Eq. (2)] and old (Ref. 21) melting-curve calibrations.

sults of Halperin *et al.* if their pressure values are uniformly shifted downward by about 10 mbar. Thus, if pressures are measured relative to $P_A = 34.3316$ bar, Eq. (2) coincides with the low-temperature calibration of Ref. 3.

On our new temperature scale we find the superconducting transition temperature for tungsten to be 15.74 ± 0.05 mK. This is 0.6 mK higher than the value originally assigned to this particular sample at the NBS. Similar discrepancies have also been detected by Lhota *et al.*[25] using the Helsinki Pt-NMR (NMR stands for nuclear magnetic resonance) temperature scale. We also note that very recently the NBS detected an error in the method they used to transfer their temperature scale to the superconducting fixed-point devices. They[26] now assign a higher value to our W sample which agrees much better with our determination. Therefore our CMN scale, the Pt-NMR scale, and the scale based on noise and nuclear orientation thermometry are all in excellent agreement—at least at 15 mK.

D. Specific-heat measurements

The heat-capacity measurements were made using the conventional heat-pulse technique: With the heat switch open the temperature of the cell was monitored to determine the equilibrium drift rate. A known amount of energy was then delivered to the cell by passing a constant current through the cell heater for a measured period of time. After thermal equilibrium was reestablished the temperature drift rate was again monitored. The change in temperature due to the heat pulse was determined by extrapolating the initial and final drifts to the middle of the heating interval. Near 10 mK, 40 min were required for each heat-capacity measurement.

For $T \lesssim 20$ mK, the drift was toward higher temperatures due to the parasitic heat leak (3 nW) into the calorimeter. At higher temperatures the drift rates were adjusted by raising and controlling the temperature of the mixing chamber. During the first half of the experiment in which measurements were made at several molar volumes but only below 0.5 K the mixing chamber was never warmed above 300 mK. This was to guard against freeing the plug of solid ^{3}He in the melting-curve—thermometer capillary. The data between 300 and 500 mK were thus obtained with negative initial and final temperature drifts which were exaggerated by the increasing conductance of the heat switch. The data between 0.4 and 2.5 K were obtained after the heat switch was removed from the cryostat and replaced with a fine copper wire.

At the lowest temperatures the precision of the data was determined by the uncertainty in the extrapolations of the temperature to the center of the heating interval. However, as the temperature increased and the thermal time constants decreased it was the resolution of the thermometers which finally limited the precision. Figure 4 shows the estimated relative uncertainty in the C_V data obtained with each of the thermometers, assuming $\Delta T \approx 0.05T$. This was the size of the temperature steps used for $T \gtrsim 30$ mK. At lower temperatures 10% steps were actually used to improve the precision of the data. Note that since the specific heat is nearly linear in temperature the errors (curvature corrections) introduced by taking these relatively large temperature steps are insignificant. At a temperature of 150 mK we switched from the melting-curve thermometer to the carbon thermometer. The precision of the data obtained above 0.4 K using the carbon resistor was improved by increasing the excitation voltage of the bridge by a factor of 4.

Aside from errors in the temperature scale, the overall accuracy of the specific-heat data is mainly influenced by the accuracy of the energy measurement and by the accuracy of the number of moles of sample determination. Considering first the energy measurement: The magnitude of the current, which was provided by an electronic constant current

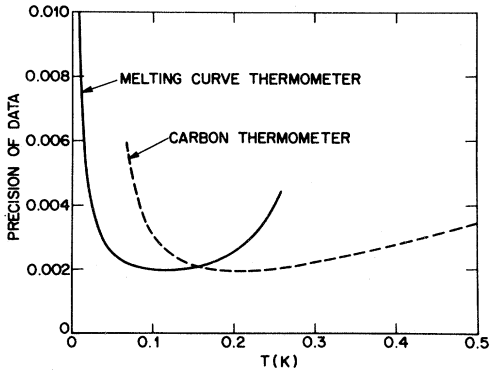

FIG. 4. Estimates of the precision of the specific-heat data obtained using the melting-curve and the carbon thermometers. Curves are based on a temperature step size of $0.05T$.

source, was accurately inferred by measuring (using a potentiometer) the voltage drop across a standard resistor in series with the heater. A relay with mercury-wetted contacts was used to switch the current from a dummy load resistor to the heater. A second pair of contacts in the relay which opened and closed within 0.2 msec of the first pair was used to trigger an electronic timer in order to accurately determine the duration of the current pulse. The resistance of the heater was known from a four-lead measurement. The total error in the energy measurement is expected to be considerably less than 0.1%. We note that changing the current and/or the heating times did not affect the results. Normally the currents were set so that the pulse lengths could be kept between 60 and 200 sec.

The ^{3}He samples were confined to constant volume using the valve mounted on the mixing chamber of the refrigerator (see Fig. 1). The valve was slowly closed with the calorimeter and mixing chamber kept very near 100 mK and with the pressure held constant using a dead-weight tester (except for $P \approx 0$). Molar volumes were then obtained using the relation

$$V_M(0.1\ \mathrm{K}) = \sum_{i=0}^{5} a_i P^i , \tag{3}$$

with

$$a_0 = 36.820,\quad a_1 = -1.2094 ,$$
$$a_2 = 9.4231\times 10^{-2},\quad a_3 = -4.9875\times 10^{-3} ,$$
$$a_4 = 1.3746\times 10^{-4},\quad a_5 = -1.4756\times 10^{-6} .$$

P is in units of bar and V_M in units of cm^3. Equation (3) gives the molar volume (at $T=0.1$ K) determined by Kerr and Taylor[27] at $P=0$ and the value inferred by Grilly[28] on the melting curve. At intermediate pressures Eq. (3) is a least-squares fit (rms deviation $=0.02$ cm^3) to the corrected[29] data of Sherman and Edeskuty[30] extended to 0.1 K using the relative density measurements of Boghosian, Meyer, and Rives.[31] The data of Abraham and Osborne[32] are consistent with these values. The number of moles of ^{3}He in the calorimeter was then simply calculated using V_M and the volume of the cell.

The cell volume was accurately measured by first filling the cell with ^{3}He at 1.6 K and at a pressure only slightly above the saturated vapor pressure, and by then quickly warming the cell to near room temperature and collecting the sample in a calibrated 4-l glass volume. For this volume-calibration run, the filling capillary was routed around the cold valve and passed through the ^{4}He bath inside an evacuated tube. The capillary was heated inside this vacuum jacket to minimize the amount of ^{3}He outside of the cell. With the use of the ^{3}He molar volume data of Kerr and Taylor[27] it is estimated that the cell-volume measurement is accurate to within 0.2%.

E. Heat capacity of the empty calorimeter

Before admitting ^{3}He to either the sample chamber or to the melting-curve thermometer, the heat capacity of the calorimeter was measured using the carbon resistor (Sec. II B). These results are indicated by the dashed curve in Fig. 5(a). The data were not extended to higher temperature because the temperature drift rates became too large for meaningful measurements to be made. This was a consequence of the increasing thermal conductance of the tin heat switch and the very small heat capacity of the silver calorimeter. There was no evidence of any unexpected contributions to the heat capacity.

The heat capacity measured with the melting-curve thermometer filled (0.1 cm^3) but with the sample chamber still evacuated is shown by the open circles in Fig. 5(a). This is the addendum to be subtracted from the total heat capacity measured with the cell filled with ^{3}He. The solid curve is a least-squares fit of the data:

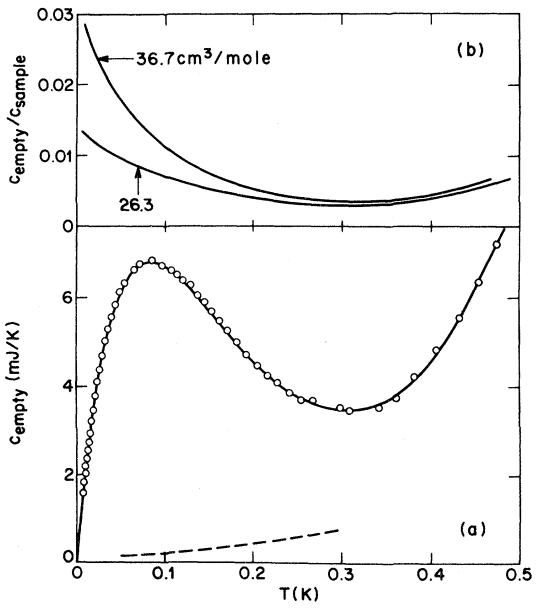

FIG. 5. (a) Addendum heat capacity measured before ^{3}He was admitted to the sample chamber. Dashed curve was measured using the carbon thermometer prior to filling the melting-curve thermometer with ^{3}He. (b) Ratio of the addendum to the sample heat capacity for two sample densities.

$$c_{\text{empty}} = \sum_{i=1}^{8} a_i T^i, \quad a_1 = 223.807 ,$$
$$a_2 = -2719.01, \quad a_3 = 16262.2 ,$$
$$a_4 = -60058.9, \quad a_5 = 146901.0 , \qquad (4)$$
$$a_6 = -236211.0, \quad a_7 = 230955.0 ,$$
$$a_8 = -104264.0 .$$

The rms deviation is ~2%. Since the heat capacity of the thermometer is dominated by the *liquid* ^{3}He contribution, the results tend toward a linear temperature dependence at low temperature. The minimum near 0.3 K corresponds to the region in which the largest fraction of ^{3}He has been converted to solid.

The ratio of the addendum heat capacity to the sample heat capacity is shown in Fig. 5(b). The two molar volumes correspond to nominal sample pressures of 0 and 29 bar. It is seen then that in the worst case this ratio is 3%. Consequently, the 2% uncertainty in the addendum has only a negligible effect on the final results.

III. RESULTS AND DISCUSSION

A. General results

The specific heat of normal liquid ^{3}He was measured with high precision along several isochores corresponding to sample pressures between 0 and 32.5 bar and over the temperature range 7 mK to 2.5 K. These data were obtained in two sets: First, measurements were made in the temperature range 7 to 500 mK, and then after minor modification of the apparatus, in the range 0.4 to 2.5 K. The molar volumes of the samples are listed in Table III.

The qualitative features of the results over the whole temperature range are shown in Fig. 6 where smoothed curves for the molar specific heat C_V divided by the gas constant R are plotted at two molar volumes corresponding to $P \approx 0$ (36.8 cm^3/mole) and to $P \approx 29$ bar (26.2 cm^3/mole). For comparison the long-dashed curves are the ideal Fermi-gas specific heat at the same two densities. In the degeneracy region at very low temperatures ($T \ll T_F$) the ideal gas specific heat is linear in T and is given by

$$\frac{C_V}{R} = \frac{\pi^2}{2}\frac{T}{T_F} , \qquad (5)$$

with

$$T_F = \frac{\hbar^2}{2m_3 k_B}\left[\frac{3\pi^2 N}{V}\right]^{2/3} = 54.91 V^{-2/3} . \qquad (6)$$

TABLE III. Molar volumes of the ^{3}He samples.

Sample	Nominal pressure (bar)	Molar volume (cm^3)	Temperature range (K)
1	0	36.743	0.007–0.5
2	5	32.566	0.007–0.5
3	11	30.054	0.007–0.5
4	17	28.373	0.007–0.5
5	22	27.270	0.007–0.5
6	29	26.270	0.007–0.5
7	32	25.672	0.007–0.5
8	0	36.260	0.4–2.5
9	5	32.512	0.4–2.5
10	11	30.014	0.4–2.5
11	17	28.304	0.4–2.5
12	22	27.222	0.4–2.5
13	29	26.200	0.4–2.5

The lack of even qualitative agreement between these two sets of curves is a clear demonstration that liquid ^{3}He must be treated as a strongly interacting system.

According to the Landau theory, which applies at very low temperatures, the ^{3}He-^{3}He interactions

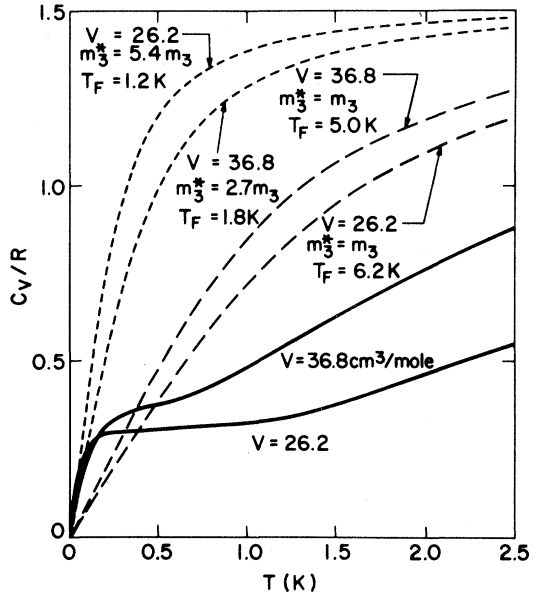

FIG. 6. Smoothed results for the ^{3}He specific heat (in units of the gas constant R) measured at molar volumes corresponding to nominal sample pressures of 0 and 29 bar. For comparison, long-dashed curves show the ideal-Fermi-gas specific heat at the same two densities. Short-dashed curves were also computed using the ideal-gas relations but with the particle mass adjusted to give the correct limiting slopes at $T = 0$.

modify the specific heat only through the renormalization of the ^{3}He mass. That is, Eqs. (5) and (6) remain valid but with the mass m_3 replaced with an effective mass m_3^*. The two short-dashed curves in Fig. 6 were determined using the noninteracting-gas relations and effective masses adjusted to give the correct limiting low-temperature dependences. Departures from these curves become apparent already at temperatures on the order of 50 mK. Therefore, to accurately describe the data at low but finite temperature requires modifications to the Landau theory which will be discussed, however, in Sec. III D. We return now to present the experimental data in more detail.

B. Empirical equations describing the C_V data

Empirical equations were found which accurately describe both the temperature and density dependence of the C_V data. These expressions are particularly useful in deriving other thermodynamic quantities. In addition, they facilitate the comparison with other experimental results obtained at intermediate densities. Unfortunately, we were unable to find a single function that was adequate over the whole temperature range (i.e., between 7 mK and 2.5 K). Instead we have two functions,

$$C_V=\sum_{\substack{i=1\\j=0}} a_{ij}V^{-j}T^{i} \tag{7}$$

and

$$C_V=\sum_{\substack{i=0\\j=0}} b_{ij}V^{j}T^{-i} + \exp\left[-T^{-1}\sum_{j} d_j V^{j}\right]\sum_{\substack{i=1\\j=0}} c_{ij}V^{j}T^{-i}, \tag{8}$$

which apply below and above 100 mK, respectively. The parameters describing the best fits of the more than 300 points below 100 mK and of the more than 400 points above 100 mK are listed in Table IV. In both cases the rms deviations are less than 0.5%.

The relative deviations of the data from Eqs. (7) and (8) are plotted in Fig. 7. At the lowest temperatures the figure shows that the precision of the data is $\pm 1\%$. However, above ~ 15 mK the precision has already improved to a few tenths of a percent and above ~ 100 mK to about 0.1%. In addition there are systematic deviations from Eq. (8) which become as large as 1% at the higher temperatures.

The smoothed C_V results at several molar volumes (corresponding to nominal sample pressures that are multiples of 5 bar) are plotted in Fig. 8 relative to the results at 36.82 cm^3/mole ($P\approx 0$). The figure shows that as the pressure is raised from 0 to 30 bar, the specific heat increases by 55% at very low temperatures, is unchanged at 160 mK, and decreases by 15% at 300 mK. It is unclear if any special significance should be attached to the finding that, to within the precision of the measurements and consistent with earlier experiments,[8] the specific heat at 160 mK is independent of density. Figure 8

TABLE IV. Best-fit parameters for Eqs. (7) and (8).

j	0	1	2	3
a_{1j}	$-2.919\,0414$	$5.289\,3401\times10^{2}$	$-1.886\,9641\times10^{4}$	$2.603\,1315\times10^{5}$
a_{3j}	$-2.475\,2597\times10^{3}$	$1.837\,7260\times10^{5}$	$-3.494\,6553\times10^{6}$	
a_{4j}	$3.888\,7481\times10^{4}$	$-2.864\,9769\times10^{6}$	$5.252\,6785\times10^{7}$	
a_{5j}	$-1.750\,5655\times10^{5}$	$1.280\,9001\times10^{7}$	$-2.303\,7701\times10^{8}$	
b_{0j}	$-6.552\,1193\times10^{-2}$	$1.350\,2371\times10^{-2}$		
b_{1j}	$4.135\,9033\times10^{-2}$	$3.823\,3755\times10^{-4}$	$-5.346\,8396\times10^{-5}$	
b_{2j}	$5.797\,6786\times10^{-3}$	$-6.561\,1532\times10^{-4}$	$1.268\,9707\times10^{-5}$	
b_{3j}	$-3.837\,4623\times10^{-4}$	$3.207\,2581\times10^{-5}$	$-5.303\,8906\times10^{-7}$	
c_{1j}	$-2.548\,2958\times10^{1}$	$1.641\,6936$	$-1.511\,0378\times10^{-2}$	
c_{2j}	$3.788\,2751\times10^{1}$	$-2.876\,9188$	$3.575\,1181\times10^{-2}$	
c_{3j}	$2.441\,2956\times10^{1}$	$-2.424\,4083$	$6.777\,5905\times10^{-2}$	
d_j	$-7.161\,3436$	$6.052\,5139\times10^{-1}$	$-7.129\,5855\times10^{-3}$	

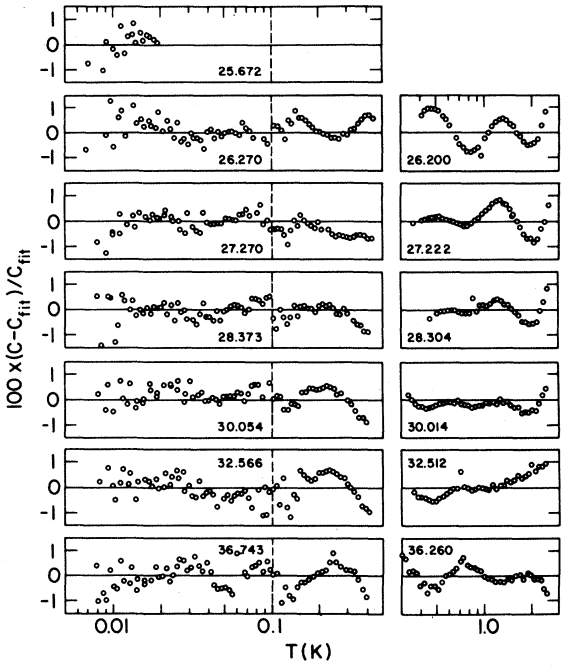

FIG. 7. Deviations from least-squares fits to the specific-heat data. Equation (7) was used below 100 mK and Eq. (8) above 100 mK. Numbers give the molar volume in cm^3. Best-fit parameters are listed in Table IV.

also shows clearly that $C_V \propto T$ only in the limit $T \to 0$ and that at a given temperature higher-order terms become progressively more important as the pressure is increased.

The smoothed C_V results above 160 mK are plotted in Fig. 9. The small bump that develops near 0.5 K at the highest pressures is also seen in the data and is not an artifact of the least-squares fits. With

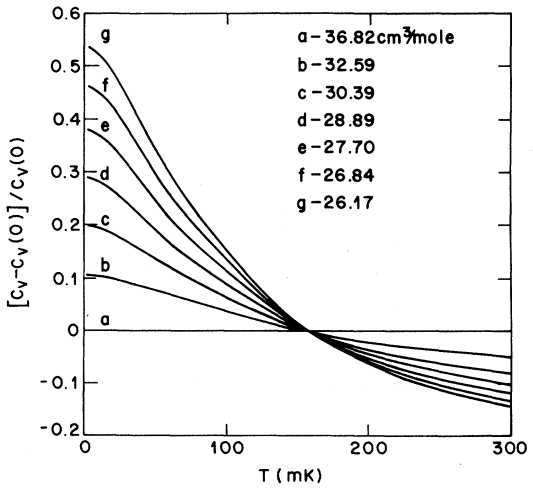

FIG. 8. Specific heat at several molar volumes plotted relative to the results at 36.82 cm^3/mole ($P \approx 0$).

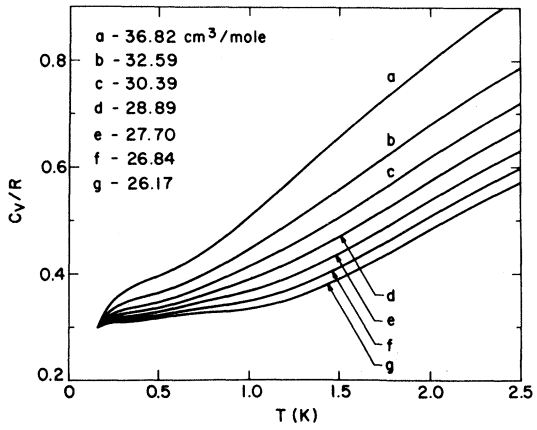

FIG. 9. High-temperature specific-heat results at several molar volumes.

the use of Eqs. (7) and (8) it is straightforward to determine several other thermodynamic quantities. For example, analytic expressions for the entropy result directly from the relation

$$S(T) = \int_0^T C_V/T\,dT\ . \tag{9}$$

A plot of the entropy versus temperature at a molar volume of 36.82 cm^3 is given in Fig. 10. The molar volume dependence of S is shown in Fig. 11 where the entropy relative to its value at vapor pressure is plotted along several isotherms. The derivative $(\partial P/\partial T)_V$ is determined by the thermodynamic identity

$$\left[\frac{\partial P}{\partial T}\right]_V = \left[\frac{\partial S}{\partial V}\right]_T . \tag{10}$$

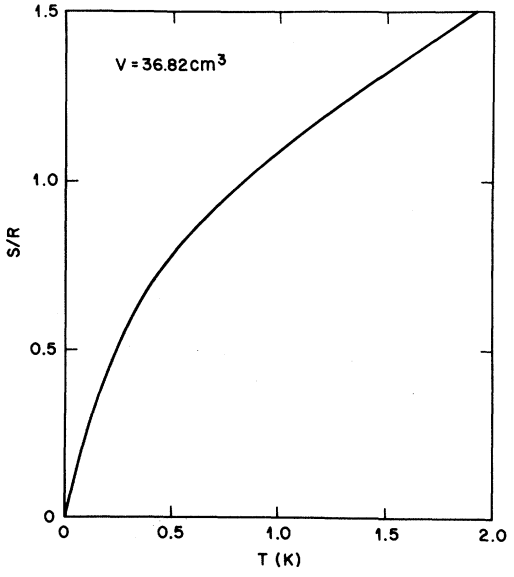

FIG. 10. ^{3}He entropy at a molar volume of 36.82 cm^3.

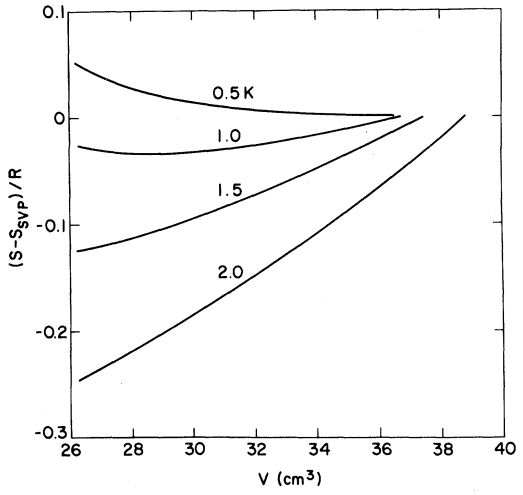

FIG. 11. Change in entropy along isotherms.

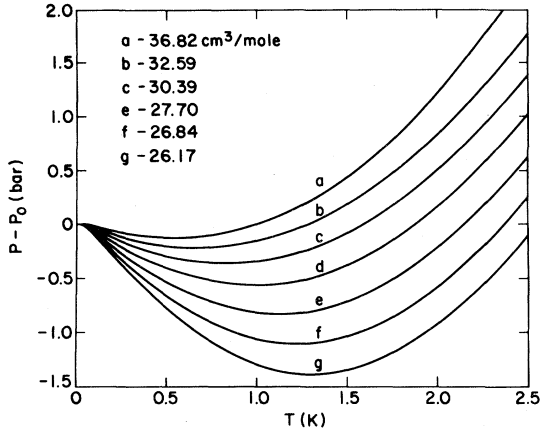

FIG. 13. Change in pressure along several isochores.

Results along several isochores are plotted in Fig. 12. Numerical integration of these values then gives the total change in pressure along isochores. Figure 13 shows that the pressure of a sample confined to constant volume changes by as much as 2 bar between 0 and 2.5 K. The minima in these curves $[(\partial P/\partial T)_V=0$ in Fig. 12] correspond to points at which the expansion coefficient is zero. The T-V coordinates agree reasonably well with other determinations.[30–33] Values of the various thermodynamic functions derived using Eqs. (7) and (8) are listed in Table V.

C. Low-temperature results

The specific-heat data below 50 mK are plotted in Fig. 14 as C_V/RT vs T. When plotted in this manner the results according to Landau theory should tend towards a constant value as $T\rightarrow 0$. At $P=0$ this behavior was guaranteed by our calibration of the ^{3}He melting curve (Sec. II C). However, based on this calibration the data at *all* pressures are found to be consistent with this expectation. The solid curves in Fig. 14 are least-squares fits of the data with the function

$$C_V/R=\gamma T+bT^3+cT^5 . \tag{11}$$

The numbers give the pressure at 0.1 K in bar. In Fig. 15 the best-fit values of γ are plotted as a function of the density. Drawn through the points is the curve which corresponds to the fit [Eq. (7)] in which the data at all densities were treated simultaneously. The comparison with the previous determinations of γ shows the unexplained wide range of results that have been extracted from specific-heat experiments with estimated accuracies of typically 2% or 3%. We find the best agreement with the γ value determined by Halperin *et al.*[3] (solid square) from measurements along the melting curve. The uncertainty in their value is ±4%. The next set of data (open circles) which comes closest to our findings is due to Anderson, Reese, and Wheatley.[4] However, the more recent and presumably more accurate measurements of Wheatley and co-workers (Abel *et al.*[5] and Mota *et al.*[6]) are shown by the open and solid diamonds at the density extremes. These data are ~10% higher than our values, but at the higher density are in good agreement with the determination by Hebral *et al.*[7] (open triangle). Falling ~20% below our results are the most recent specific-heat measurements made by Haavasoja *et al.*[1] (open squares) and by Zeise *et al.*[2] (solid triangles). In both of these experiments data was obtained only for $T\lesssim 10$ mK. It might also be noted

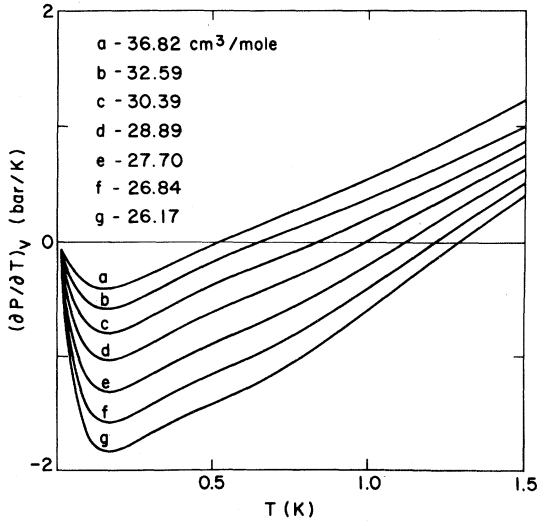

FIG. 12. Derivative $(\partial P/\partial T)_V$ along several isochores.

TABLE V. Smoothed thermodynamic functions for normal liquid ^{3}He. Note that for nominal pressures of 0 and 30 bar some of the listings have P-T coordinates below the vapor curve or above the melting curve, respectively.

T (K)	C_V/R	S/R	$(\partial P/\partial T)_V$ (bar/K)	$P(T)-P(0)$ (bar)	T (K)	C_V/R	S/R	$(\partial P/\partial T)_V$ (bar/K)	$P(T)-P(0)$ (bar)
		$V=36.820$					$V=32.587$		
		$P(0.1\ \text{K})=0.0$					$P(0.1\ \text{K})=5.0$		
0.005	0.0137	0.0137	−0.0245	−0.0001	0.005	0.0153	0.0153	−0.0415	−0.0001
0.010	0.0274	0.0274	−0.0489	−0.0002	0.010	0.0305	0.0306	−0.0824	−0.0004
0.020	0.0543	0.0547	−0.0971	−0.0010	0.020	0.0604	0.0610	−0.1610	−0.0016
0.040	0.1056	0.1083	−0.1882	−0.0038	0.040	0.1157	0.1202	−0.2973	−0.0063
0.060	0.1511	0.1600	−0.2681	−0.0084	0.060	0.1630	0.1764	−0.4008	−0.0133
0.080	0.1899	0.2089	−0.3336	−0.0145	0.080	0.2016	0.2288	−0.4745	−0.0221
0.100	0.2235	0.2550	−0.3850	−0.0217	0.100	0.2323	0.2773	−0.5243	−0.0321
0.150	0.2897	0.3593	−0.4085	−0.0417	0.150	0.2902	0.3837	−0.5829	−0.0603
0.200	0.3272	0.4483	−0.3863	−0.0618	0.200	0.3193	0.4717	−0.5635	−0.0891
0.250	0.3499	0.5240	−0.3391	−0.0800	0.250	0.3352	0.5448	−0.5112	−0.1161
0.300	0.3648	0.5892	−0.2801	−0.0955	0.300	0.3449	0.6068	−0.4457	−0.1400
0.350	0.3754	0.6462	−0.2164	−0.1079	0.350	0.3513	0.6605	−0.3758	−0.1606
0.400	0.3834	0.6969	−0.1516	−0.1171	0.400	0.3562	0.7077	−0.3059	−0.1776
0.450	0.3901	0.7425	−0.0877	−0.1231	0.450	0.3605	0.7499	−0.2384	−0.1912
0.500	0.3966	0.7839	−0.0256	−0.1259	0.500	0.3651	0.7881	−0.1745	−0.2015
0.600	0.4110	0.8574	0.0923	−0.1255	0.600	0.3765	0.8557	−0.0571	−0.2130
0.700	0.4296	0.9221	0.2045	−0.1076	0.700	0.3912	0.9148	0.0509	−0.2133
0.800	0.4525	0.9809	0.3160	−0.0816	0.800	0.4085	0.9681	0.1565	−0.2025
0.900	0.4787	1.0357	0.4309	−0.0443	0.900	0.4274	1.0173	0.2648	−0.1819
1.000	0.5070	1.0876	0.5515	0.0048	1.000	0.4473	1.0634	0.3781	−0.1498
1.200	0.5660	1.1852	0.8098	0.1405	1.200	0.4893	1.1486	0.6178	−0.0504
1.400	0.6257	1.2770	1.0834	0.3297	1.400	0.5340	1.2273	0.8663	0.0979
1.600	0.6845	1.3644	1.3608	0.5731	1.600	0.5808	1.3017	1.1132	0.2963
1.800	0.7417	1.4483	1.6337	0.8737	1.800	0.6287	1.3729	1.3526	0.5427
2.000	0.7965	1.5293	1.8973	1.2270	2.000	0.6760	1.4416	1.5823	0.8363
2.500	0.9191	1.7206	2.5040	2.3305	2.500	0.7853	1.6045	2.1132	1.7627
		$V=30.389$					$V=28.887$		
		$P\ (0.1\ \text{K})=10.0$					$P\ (0.1\ \text{K})=15.0$		
0.005	0.0166	0.0166	−0.0596	−0.0001	0.005	0.0179	0.0179	−0.0787	−0.0002
0.010	0.0331	0.0332	−0.1182	−0.0006	0.010	0.0355	0.0357	−0.1560	−0.0008
0.020	0.0651	0.0661	−0.2298	−0.0023	0.020	0.0695	0.0708	−0.3030	−0.0031
0.040	0.1231	0.1295	−0.4189	−0.0089	0.040	0.1298	0.1382	−0.5503	−0.0117
0.060	0.1709	0.1888	−0.5570	−0.0188	0.060	0.1780	0.2004	−0.7298	−0.0246
0.080	0.2088	0.2434	−0.6525	−0.0309	0.080	0.2154	0.2569	−0.8552	−0.0406
0.100	0.2397	0.2934	−0.7163	−0.0446	0.100	0.2459	0.3082	−0.9419	−0.0586

TABLE V. (*Continued.*)

T (K)	C_V/R	S/R	$(\partial P/\partial T)_V$ (bar/K)	$P(T)-P(0)$ (bar)	T (K)	C_V/R	S/R	$(\partial P/\partial T)_V$ (bar/K)	$P(T)-P(0)$ (bar)
		$V=30.389$					$V=28.887$		
		$P(0.1\ \text{K})=10.0$					$P(0.1\ \text{K})=15.0$		
0.150	0.2911	0.4017	−0.7931	−0.0830	0.150	0.2920	0.4180	−1.0311	−0.1086
0.200	0.3149	0.4891	−0.7752	−0.1224	0.200	0.3118	0.5051	−1.0141	−0.1600
0.250	0.3269	0.5608	−0.7203	−0.1599	0.250	0.3210	0.5758	−0.9575	−0.2094
0.300	0.3337	0.6210	−0.6514	−0.1942	0.300	0.3258	0.6348	−0.8865	−0.2555
0.350	0.3380	0.6728	−0.5786	−0.2250	0.350	0.3287	0.6852	−0.8122	−0.2980
0.400	0.3414	0.7182	−0.5069	−0.2521	0.400	0.3313	0.7293	−0.7400	−0.3369
0.450	0.3448	0.7586	−0.4387	−0.2757	0.450	0.3341	0.7685	−0.6722	−0.3720
0.500	0.3488	0.7951	−0.3749	−0.2960	0.500	0.3377	0.8038	−0.6094	−0.4041
0.600	0.3589	0.8595	−0.2587	−0.3276	0.600	0.3468	0.8662	−0.4938	−0.4592
0.700	0.3715	0.9158	−0.1499	−0.3480	0.700	0.3574	0.9204	−0.3806	−0.5029
0.800	0.3855	0.9663	−0.0395	−0.3575	0.800	0.3684	0.9689	−0.2601	−0.5352
0.900	0.4002	1.0126	0.0771	−0.3557	0.900	0.3795	1.0129	−0.1292	−0.5546
1.000	0.4156	1.0555	0.2007	−0.3419	1.000	0.3913	1.0535	0.0107	−0.5606
1.200	0.4490	1.1342	0.4620	−0.2758	1.200	0.4186	1.1272	0.3049	−0.5292
1.400	0.4869	1.2062	0.7283	−0.1568	1.400	0.4519	1.1941	0.6000	−0.4386
1.600	0.5285	1.2739	0.9883	0.0151	1.600	0.4903	1.2569	0.8836	−0.2901
1.800	0.5722	1.3386	1.2371	0.2378	1.800	0.5315	1.3170	1.1521	−0.0861
2.000	0.6162	1.4012	1.4739	0.5091	2.000	0.5732	1.3752	1.4062	0.1699
2.500	0.7182	1.5500	2.0203	1.3851	2.500	0.6698	1.5138	1.9910	1.0218
		$V=27.696$					$V=26.835$		
		$P(0.1\ \text{K})=20.0$					$P(0.1\ \text{K})=25.0$		
0.005	0.0191	0.0191	−0.0996	−0.0002	0.005	0.0202	0.0203	−0.1192	−0.0003
0.010	0.0380	0.0382	−0.1976	−0.0010	0.010	0.0402	0.0404	−0.2364	−0.0012
0.020	0.0741	0.0757	−0.3836	−0.0039	0.020	0.0781	0.0801	−0.4590	−0.0047
0.040	0.1367	0.1471	−0.6967	−0.0149	0.040	0.1428	0.1550	−0.8346	−0.0178
0.060	0.1852	0.2121	−0.9253	−0.0312	0.060	0.1918	0.2226	−1.1113	−0.0374
0.080	0.2223	0.2707	−1.0884	−0.0514	0.080	0.2287	0.2831	−1.3126	−0.0617
0.100	0.2515	0.3235	−1.2059	−0.0745	0.100	0.2558	0.3373	−1.4626	−0.0896
0.150	0.2929	0.4346	−1.3050	−0.1380	0.150	0.2937	0.4494	−1.5688	−0.1662
0.200	0.3093	0.5215	−1.2888	−0.2031	0.200	0.3075	0.5361	−1.5533	−0.2445
0.250	0.3162	0.5913	−1.2308	−0.2662	0.250	0.3127	0.6054	−1.4943	−0.3208
0.300	0.3194	0.6493	−1.1584	−0.3259	0.300	0.3147	0.6626	−1.4211	−0.3937
0.350	0.3213	0.6987	−1.0835	−0.3820	0.350	0.3160	0.7112	−1.3464	−0.4629
0.400	0.3233	0.7417	−1.0118	−0.4343	0.400	0.3176	0.7535	−1.2761	−0.5284
0.450	0.3258	0.7799	−0.9454	−0.4832	0.450	0.3200	0.7910	−1.2115	−0.5906

TABLE V. (*Continued.*)

T (K)	C_V/R	S/R	$(\partial P/\partial T)_V$ (bar/K)	$P(T)-P(0)$ (bar)	T (K)	C_V/R	S/R	$(\partial P/\partial T)_V$ (bar/K)	$P(T)-P(0)$ (bar)
		$V=27.696$					$V=26.835$		
		$P(0.1\ \text{K})=20.0$					$P(0.1\ \text{K})=25.0$		
0.500	0.3291	0.8144	−0.8839	−0.5290	0.500	0.3230	0.8249	−1.1512	−0.6496
0.600	0.3370	0.8751	−0.7676	−0.6115	0.600	0.3296	0.8844	−1.0329	−0.7589
0.700	0.3453	0.9277	−0.6463	−0.6823	0.700	0.3356	0.9356	−0.9019	−0.8558
0.800	0.3531	0.9743	−0.5111	−0.7403	0.800	0.3405	0.9808	−0.7508	−0.9386
0.900	0.3608	1.0163	−0.3613	−0.7840	0.900	0.3454	1.0212	−0.5815	−1.0053
1.000	0.3694	1.0548	−0.2006	−0.8122	1.000	0.3513	1.0579	−0.4004	−1.0545
1.200	0.3915	1.1240	0.1341	−0.8190	1.200	0.3695	1.1234	−0.0268	−1.0972
1.400	0.4213	1.1865	0.4641	−0.7589	1.400	0.3968	1.1823	0.3366	−1.0659
1.600	0.4572	1.2450	0.7771	−0.6345	1.600	0.4310	1.2374	0.6780	−0.9641
1.800	0.4964	1.3011	1.0710	−0.4493	1.800	0.4688	1.2904	0.9968	−0.7962
2.000	0.5363	1.3555	1.3478	−0.2072	2.000	0.5073	1.3418	1.2963	−0.5666
2.500	0.6284	1.4853	1.9838	0.6286	2.500	0.5959	1.4648	1.9833	0.2564
				$V=26.169$					
				$P(0.1\ \text{K})=30.0$					
0.005	0.0213	0.0213	−0.1375	−0.0003	0.450	0.3156	0.8017	−1.4688	−0.6937
0.010	0.0421	0.0425	−0.2728	−0.0014	0.500	0.3183	0.8351	−1.4097	−0.7663
0.020	0.0818	0.0840	−0.5298	−0.0054	0.600	0.3236	0.8936	−1.2886	−0.9007
0.040	0.1484	0.1622	−0.9648	−0.0205	0.700	0.3273	0.9438	−1.1471	−1.0226
0.060	0.1979	0.2322	−1.2880	−0.0432	0.800	0.3296	0.9877	−0.9798	−1.1301
0.080	0.2348	0.2945	−1.5274	−0.0715	0.900	0.3320	1.0266	−0.7916	−1.2179
0.100	0.2594	0.3500	−1.7102	−0.1040	1.000	0.3358	1.0618	−0.5910	−1.2878
0.150	0.2943	0.4630	−1.8219	−0.1931	1.200	0.3509	1.1242	−0.1811	−1.3643
0.200	0.3061	0.5496	−1.8068	−0.2841	1.400	0.3763	1.1801	0.2134	−1.3608
0.250	0.3099	0.6183	−1.7472	−0.3731	1.600	0.4091	1.2324	0.5814	−1.2816
0.300	0.3111	0.6750	−1.6738	−0.4586	1.800	0.4457	1.2827	0.9239	−1.1298
0.350	0.3119	0.7230	−1.5999	−0.5404	2.000	0.4832	1.3316	1.2451	−0.9133
0.400	0.3133	0.7647	−1.5313	−0.6196	2.500	0.5689	1.4489	1.9812	−0.1026

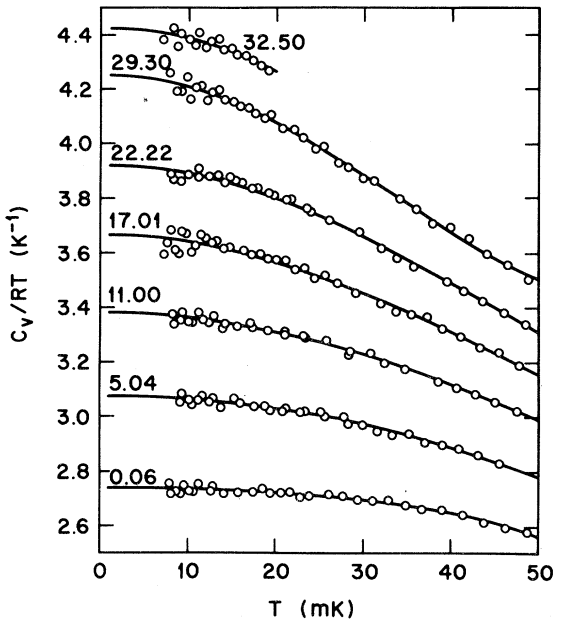

FIG. 14. Specific-heat measurements plotted as C_V/RT vs T. Numbers give the sample pressures in bars at 0.1 K. Solid curves are least-squares fits of the data using Eq. (11).

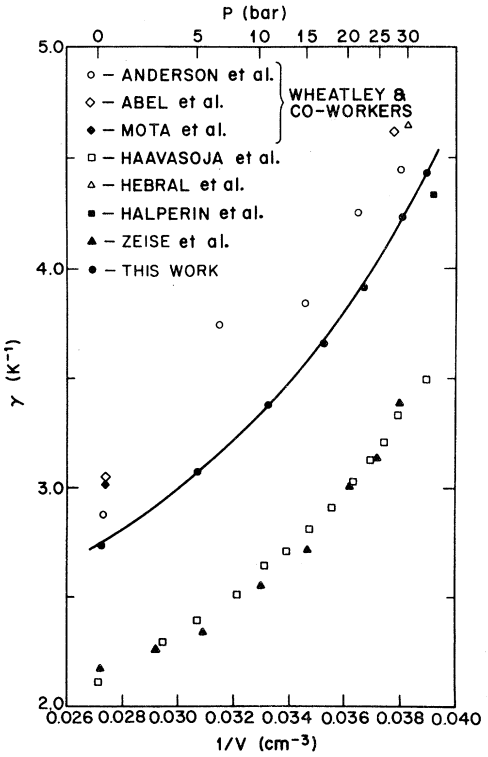

FIG. 15. Comparison of γ values derived from specific-heat measurements.

that in contrast to all of the other experiments, the calorimeter used by Zeise *et al.* was of a very unique design. The apparatus was a driven torsional oscillator whose amplitude was calibrated to give the temperature.

Although γ is a very important parameter to be extracted from the specific-heat measurements, the comparison of values derived from different experiments does not present the complete picture, and in fact can be misleading. It compares only the limiting behavior of the specific heat which is suggested by measurements at finite temperatures. Comparison of the actual measurements is made in Fig. 16. Plotted here are the fractional differences from the present results [Eqs. (7) and (8)] at the same densities. Figure 16(a) shows data obtained near $P=0$ and Fig. 16(b) shows data obtained near the melting curve. No adjustments were made for differences in C_V, C_P, and C_{SVP} since these are quite small below 0.5 K. Contrary to the situation at very low temperatures, Fig. 16 shows that all of the existing data for $T \gtrsim 30$ mK agree with the present measurements (which lie about midway in the scatter of results) to within roughly $\pm 5\%$. The serious discrepancies are then confined only to the region below 30 mK. In the following subsections we present arguments to show that only the present data are thermodynamically consistent with several other types of experiments.

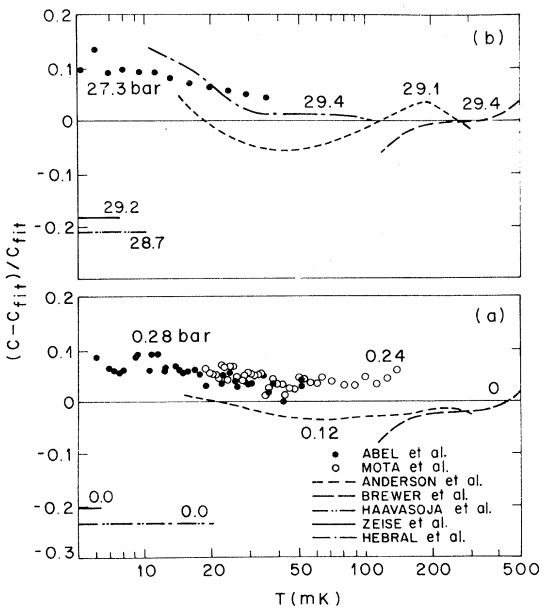

FIG. 16. Comparsion of specific-heat data obtained (a) near $P=0$, and (b) near the melting curve. C_{fit} refers to Eqs. (7) and (8) evaluated at the appropriate densities.

D. Entropy along the melting curve

Halperin *et al.*[3] measured the entropy of solid ^{3}He along the melting curve in the temperature range from below the spin-ordering transition ($T_c \approx 1$ mK) up to 20 mK. They found that for $T \approx 10$ mK the entropy is already that characterizing a fully disordered spin system, i.e., R ln2. Although at very much higher temperatures the increasing phonon and thermal-vacancy contributions to the total entropy of the solid will become significant, at 0.32 K these terms[34] are still only $\sim 0.3\%$ of the spin contribution. Thus between 10 mK and the minimum in the melting curve[21] ($T_{\min} = 0.318$ K) the total entropy of solid ^{3}He at melting should be quite accurately R ln2.

This thermodynamic information together with the Clausius-Clapeyron relation

$$\left[\frac{dP}{dT}\right]_m = \frac{S_{l,m} - S_{s,m}}{V_{l,m} - V_{s,m}} \tag{12}$$

allows us then to perform an important check on the *liquid* ^{3}He specific-heat data. The entropy of the liquid on the melting curve at temperature T_m is easily computed using the smoothed results for C_V, the $V_{l,m}$ vs T_m data of Grilly[28] and the relation

$$S_{l,m} = \int_0^{T_m(V)} \frac{C_V(V)}{T} dT \,. \tag{13}$$

These results are plotted in Fig. 17 as open circles.

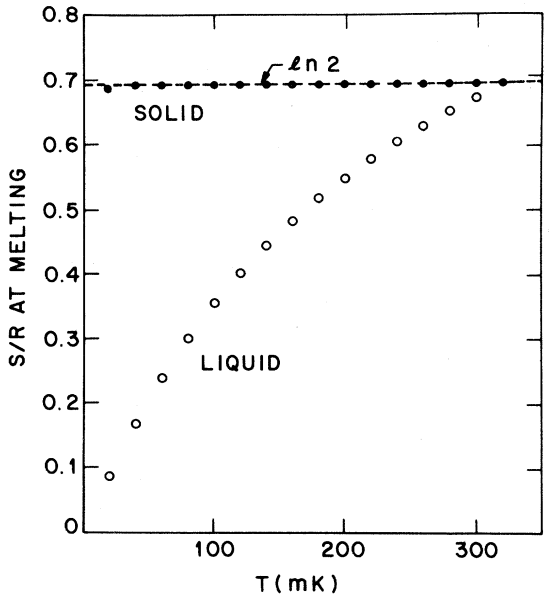

FIG. 17. Entropy of liquid and solid ^{3}He along the melting curve determined using the measured liquid specific heat and Eqs. (12) and (13).

Additionally, with the use of values of $(dP/dT)_m$ derived from Eq. (2) and values of $V_{l,m} - V_{s,m}$ from Grilly,[28] the solid entropy can be computed using Eq. (12) and compared with the R ln2. The calculated solid entropy, which ranges from a lowest value of $0.688R$ at 20 mK to a highest value of $0.693R$ at $T_{\min}$ is plotted in Fig. 17 as solid circles. The fact that we obtain a nearly constant solid entropy with a magnitude in excellent agreement with the expected value demonstrates a thermodynamic consistency between the various sets of input data. Since the specific heat and the slope of the melting curve have, by far, the strongest temperature dependences, it is these two quantities which are critically compared. We conclude then that there are no serious errors in our specific-heat measurements or in our melting-curve–temperature scale.

Looking again at Fig. 16, it is apparent that the integration of the C/T data of Abel *et al.*[5] and Mota *et al.*[6] will yield an entropy at $T_{\min}$ which is at least 5% too large. Extrapolations of the Cornell[2] and Helsinki[1] data, which unrealistically assume that the specific heat remains linear in temperature out to about 60 mK and then joins onto the present high-temperature results, lead to upper limits for S/R at $T_{\min}$ which are still about 5% too small. These discrepancies are outside of the expected experimental uncertainties.

E. Entropy at vapor pressure

Another thermodynamic check that can be made, this time on the very-low-pressure data, was recently proposed by Abraham.[35] He noted that the entropy of the liquid at SVP and at 1.5 K is known quite accurately from a determination[36] which is not based on the integration of specific-heat data. Instead it is based on a measurement of the entropy of vaporization at 1.5 K and on the calculated entropy of the *real* gas (i.e., with virial coefficients included). The result is $S/R = 1.315 \pm 0.015$. Integration of the present C_V/T data yields a corresponding value of 1.332. This favorable comparison, which stresses the higher-temperature C_V results, provides further evidence that there are no serious errors, for example, in the cell-volume determination, the energy-input measurements, or in the thermometry.

In order to be able to make a comparison with specific-heat data which do not extend to these high temperatures, Abraham integrated existing C/T data between 90 mK and 1.5 K to determine S (90 mK), noting that in this temperature range there is no question about thermal equilibrium, the background heat capacity, or the temperature scale. For this calculation he used the C_{SVP} data of Strongin *et al.*[9] and Abraham *et al.*[10] and found $S/R = 0.22$.

A reasonable error to assign to this number is ± 0.025. If the present C_V data are used instead, then S/R at 90 mK is 0.215 ± 0.018. This fine agreement demonstrates a consistency between the C_{SVP} and C_V measurements in this temperature range. It should be noted again that these values for S/R at 90 mK are independent of any temperature scale that might be used below 90 mK.

Integration of the present low-temperature data between 0 and 90 mK yields a value of 0.233 which agrees with Abraham's determination. The data of Wheatley and co-workers[5,6] give $S/R=0.25$ which is too large. Haavasoja's data extend to only 20 mK and Zeise's to only ~ 5 mK, so S/R values from these experiments depend on how the extrapolations are made to higher temperatures. Reasonable extrapolations give values less than ~ 0.19, which are too small.

F. Comparison with $P_V(T)$ data

Roach *et al.*[37] extracted information about the low-temperature ^{3}He specific heat from high-precision measurements of the pressure along isochores. At very low temperature the pressure is approximately given by the relation

$$\Delta P \equiv P(V,T)-P(V,0)=\frac{1}{2}\left[\frac{\partial^2 P}{\partial T^2}\right]_V\Bigg|_{T=0} T^2 . \tag{14}$$

The term linear in T does not appear in the expansion since

$$\left[\frac{\partial P}{\partial T}\right]_V = \left[\frac{\partial S}{\partial V}\right]_T \tag{15}$$

is identically zero at $T=0$. From Eq. (15) it also follows that

$$\left[\frac{\partial^2 P}{\partial T^2}\right]_V = \frac{1}{T}\left[\frac{\partial C_V}{\partial V}\right]_T , \tag{16}$$

which at $T=0$ is equal to $R\, d\gamma/dV$. Pressure measurements performed at very low temperatures, therefore, should yield quite directly the derivative $d\gamma/dV$. The values determined by Roach *et al.* are plotted in Fig. 18 (open circles) as a function of the nominal sample pressure. Comparison is made with the derivatives obtained from our specific-heat data (solid curve) and from the specific-heat data of Haavasoja *et al.*[1] (dashed curve). The specific-heat data of Wheatley and co-workers[4–6] are really not precise enough to determine this quantity. Assuming, however, that their results differ from ours by a multiplicative factor their curve would lie $\sim 10\%$ above the solid curve.

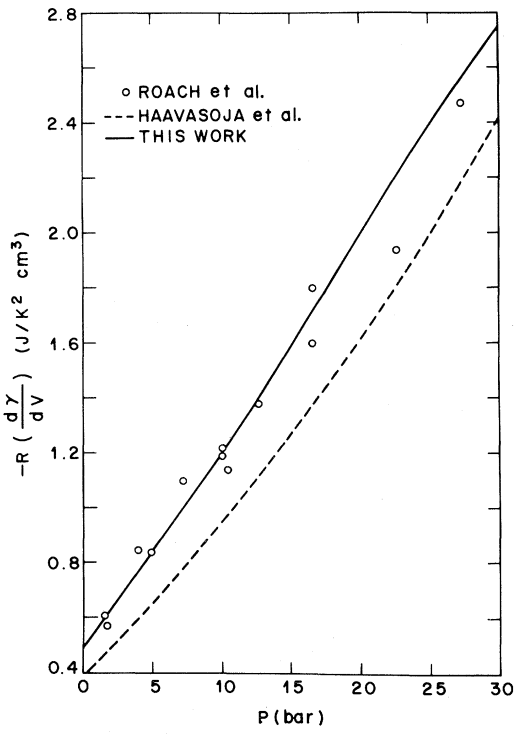

FIG. 18. Derivative $d\gamma/dV$ extracted from pressure measurements by Roach *et al.* (Ref. 37) compared with results based on specific-heat measurements.

Roach *et al.* note that, compared to specific-heat data, pressure measurements are less sensitive to the effects of heat leaks and long equilibrium times and so are less susceptible to possible errors from these sources. Such measurements, therefore, can provide an important check for calorimeter data. It must be realized though that Eq. (14) is valid only in the limit of very low temperatures. At low but finite temperatures, higher-order terms may be contributing significantly. This is demonstrated in Fig. 19. The solid curves are the isochoric-pressure changes computed for several nominal sample pressures using the relation

$$\Delta P = \int_0^T \left[\frac{\partial S}{\partial V}\right]_T dT \tag{17}$$

and the present low-temperature specific-heat results which are described by Eq. (7). Explicitly, if we write

$$C_V=\gamma T+bT^3+cT^4+dT^5 ,$$

then

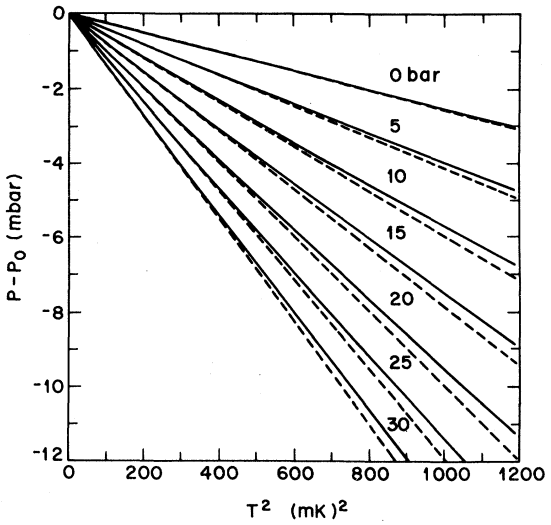

FIG. 19. Change in pressure implied by the specific-heat measurements [Eq. (18)]. Dashed lines show the limiting T^2 dependence.

$$\frac{\Delta P}{R}=\frac{1}{2}\left[\frac{\partial\gamma}{\partial V}\right]_T T^2+\frac{1}{12}\left[\frac{\partial b}{\partial V}\right]_T T^4 + \frac{1}{20}\left[\frac{\partial c}{\partial V}\right]_T T^5+\frac{1}{30}\left[\frac{\partial d}{\partial V}\right]_T T^6 . \quad (18)$$

The straight, dashed lines in Fig. 19 are extrapolations of the limiting low-temperature behavior, i.e., they correspond to only the first term of Eq. (18). Roach *et al.* analyzed their pressure data obtained over the same temperature range plotted in Fig. 19 assuming $\Delta P \propto T^2$. Consequently, their values of $|(\partial\gamma/\partial V)_T|$ must be too small by several percent. Shifting their data by this amount does not really worsen the agreement with our values (Fig. 18). It is, however, in the direction widening the discrepancy with the values of Haavasoja *et al.*

G. C_V at finite temperatures

According to the Landau Fermi-liquid theory, the specific heat of normal liqud ^{3}He should exhibit a linear temperature dependence at very low temperatures. The actual temperature range over which one might expect the theory to be valid can be estimated (from the condition that the quasiparticle lifetime be sufficiently long) to be roughly less than $0.1T_F$. But even from Fig. 6 it is already evident that significant departures from linear behavior extend down to much lower temperatures, particularly at the higher sample pressures. Theoretically this is explained as being mainly due to the coupling of the quasiparticles to the incoherent spin fluctuations.[38–41] With this coupling taken into account the specific-heat function has the form

$$C_V/R=\gamma T+\Gamma T^3\ln(T/\theta_c) . \quad (19)$$

It has been estimated[42] that this relation should be valid below about 25 mK.

Our data at all pressures, however, are consistent with an expression of this form out to considerably higher temperatures. Table VI gives values of γ, Γ, and θ_c resulting from least-squares fits of the data between 20 and 100 mK. The relative deviations of the data from the best fits are shown in Fig. 20 and a plot of Γ vs P is given in Fig. 21. Data obtained below 20 mK were not included in this analysis since they are particularly subject to the uncertainties in the CMN Δ (Sec. II C). Note though that the γ values listed in Table VI, which are more dependent on higher-temperature data, agree with those determined by Eq. (7) to within about 1%.

In Fig. 22, the $T^3\ln T$ contribution to C_V is exhibited more explicitly. Here $(\gamma-C_V/RT)/T^2$ is plotted versus $\ln T$. The data lying along straight lines in this plot demonstrates the consistency with the form of Eq. (19). If the correction to the leading term were proportional to T^3 rather than to $T^3\ln T$, the data as plotted in Fig. 22 would tend toward a

TABLE VI. Parameters resulting from least-squares fits of the specific-heat data ($20 \le T \le 100$ mK) using Eq. (19).

P (bar)	γ (K^{-1})	Γ (K^{-3})	θ_c (K)	rms deviations (%)
0.06	2.78	35.4	0.458	0.39
5.04	3.11	63.5	0.347	0.31
11.00	3.43	103.0	0.265	0.19
17.01	3.70	136.7	0.243	0.22
22.22	3.96	163.2	0.238	0.30
29.30	4.24	200.9	0.226	0.30

constant value (i.e., zero slope) with decreasing temperature.

Assuming that all of the $T^3 \ln T$ contribution to C_V comes from interactions between quasiparticles whose momenta are almost equal, Pethick and Carneiro[40] derived an expression for Γ in terms of Landau parameters. If Landau parameters with $l>1$ are neglected,

$$\Gamma=\tfrac{3}{40}(\pi^4/T_F^3)\sum_{\lambda=s,a}\omega_\lambda[(A_0^\lambda)^2(1+A_1^\lambda-\tfrac{1}{12}\pi^2A_0^\lambda)+(A_1^\lambda)^2(1-\tfrac{1}{48}\pi^2A_1^\lambda)-2A_0^\lambda A_1^\lambda]\,, \tag{20}$$

where s and a refer to symmetric and antisymmetric terms, $\omega_s=1$, $\omega_a=3$, and

$$A_l^\lambda=\frac{F_l^\lambda}{1+F_l^\lambda/(2l+1)}\,. \tag{21}$$

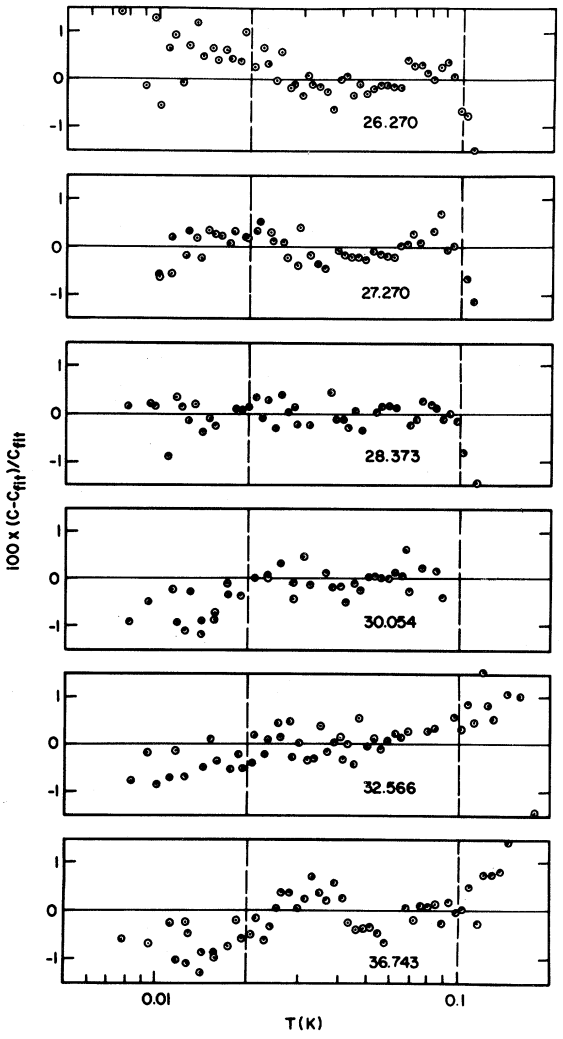

FIG. 20. Deviations from least-squares fits to the specific-heat data between 20 and 100 mK using Eq. (19). Numbers give the molar volume in cm^3. Best-fit parameters are listed in Table VI.

Since the parameter F_1^a has not been accurately determined experimentally it is not meaningful to evaluate Eq. (20) in order to make comparison with the experimental results for Γ. On the other hand, Eq. (20), in conjunction with the experimental results for Γ offers us a means of inferring values of F_1^a. For these computations F_1^s was determined using the relation

$$F_1^s=3\left[\frac{m_3^*}{m_3}-1\right] \tag{22}$$

together with γ values described by Eq. (7). Values of F_0^s and F_0^a were taken from Wheatley's[43] table but corrected for the present determination of m_3^*. All of these parameters are listed in Table VII for several sample densities. At zero pressure and at P_{melting} we obtain respective values for F_1^a of -0.55 and -0.99. These can be compared with -0.7 and -1.1 determined by Pethick *et al.*[44] from their calculations together with fits of the finite-temperature contributions to the thermal-conductivity data of Abel *et al.*[45] In this analysis, Landau parameters with $l>1$ were also neglected and m_3^*/m_3 was taken to be 3.01 (Ref. 43) at $P=0$ and 6.22 at P_{melting}. At the melting pressure, comparisons can also be made with the value inferred by Osheroff *et al.*[46] from their analysis of spin-wave velocities in the su-

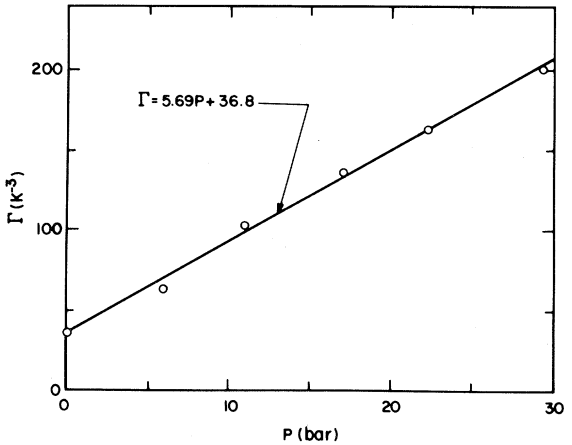

FIG. 21. Parameter Γ determined from least-squares fits of the specific-heat data using Eq. (19).

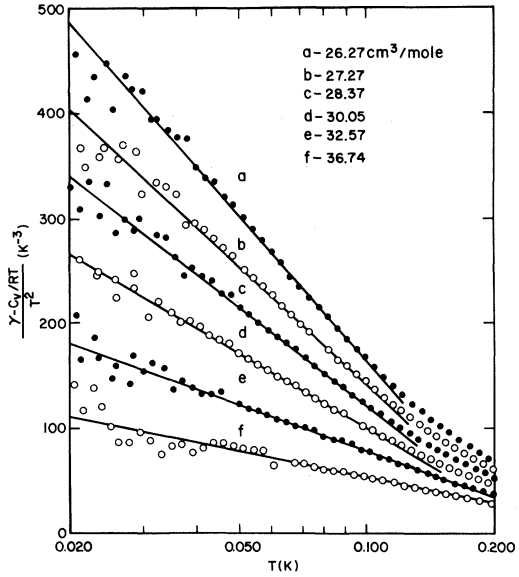

FIG. 22. Specific-heat data plotted to demonstrate the consistency with Eq. (19).

perfluid B phase. They find $F_1^a=-1.2$ using $m_3^*/m_3=5.53$.[3] Bearing in mind the approximations and uncertainties involved in obtaining F_1^a, there is fine agreement between these various determinations. This is a strong indication that the ability of Eq. (19) to fit the data, at all pressures, out to temperatures of 100 mK is not fortuitous.

Recently, there have been new attempts[47,48] to understand the specific heat at higher temperatures, i.e., at temperatures for which the low-temperature expansion Eq. (19) is no longer expected to be valid. In these calculations the departures from the Landau linear specific heat are thought of in terms of a temperature-dependent effective mass. Brown *et al.*[47] assume that almost all of the effective mass acquired by the quasiparticles is due to the coupling to the low-lying spin fluctuations. In their model m_3^*/m_3 tends towards unity with increasing temperature as the relevant collective modes are "shaken off." Consequently, the spin-fluctuation theory [Eq. (19)] remains valid at low temperatures ($T \lesssim 50$ mK) but goes over into the paramagnon theory[38,39] at higher temperatures. The theory does not predict the specific heat quantitatively but it does give the general trend of C_V with temperature correctly out to several hundred mK.

Fantoni *et al.*[48] consider the specific heat over a much larger temperature range which extends up to 2 K. With the use of a microscopic approach they show that the general features of the measured specific heat can be understood by way of a quasiparticle spectrum $\epsilon(k)$ which exhibits a wiggle at k_F. The wiggle implies a large enhancement of $m_3^*(k)=\hbar^2 k/(d\epsilon/dk)$ in a narrow region around k_F and is responsible for $m_3^*(T)$ increasing with decreasing temperature.

ACKNOWLEDGMENT

I am grateful to Paul A. Busch for his expert technical assistance.

TABLE VII. Landau parameters. Reduced mass m_3^*/m_3 and parameter F_1^s were computed using γ from Eq. (7). F_0^s and F_0^a are from Ref. 43 but corrected for the new determination of m_3^*/m_3. F_1^a is based on Eq. (20) and the relation $\Gamma=5.69P+36.8$ which fits the Γ values listed in Table VI.

P (bar)	V (cm^3)	γ (K^{-1})	m_3^*/m_3	F_1^s	F_0^s	F_0^a	Γ (K^{-3})	F_1^a
0	36.84	2.74	2.76	5.27	9.15	−0.700	36.8	−0.55
3	33.87	2.95	3.13	6.40	15.83	−0.725	53.9	−0.73
6	32.07	3.12	3.44	7.32	22.22	−0.736	71.0	−0.79
9	30.76	3.28	3.72	8.15	28.61	−0.745	88.1	−0.86
12	29.71	3.43	3.98	8.95	34.97	−0.750	105.0	−0.90
15	28.86	3.58	4.24	9.71	41.33	−0.755	122.0	−0.95
18	28.13	3.73	4.49	10.47	48.03	−0.759	139.0	−0.99
21	27.56	3.87	4.71	11.14	54.37	−0.759	156.0	−0.99
24	27.06	4.00	4.93	11.80	61.02	−0.760	173.0	−1.00
27	26.58	4.13	5.17	12.50	68.22	−0.759	190.0	−0.99
30	26.14	4.27	5.40	13.20	75.60	−0.758	208.0	−0.98
33	25.71	4.42	5.65	13.96	83.44	−0.759	225.0	−1.01
34.36	25.54	4.49	5.76	14.28	87.09	−0.757	232.0	−0.99

[1]T. Haavasoja, Ph.D. thesis, Helsinki University of Technology, 1980 (unpublished); T. A. Alvesalo, T. Haavasoja, and M. T. Manninen, J. Low Temp. Phys. 45, 373 (1981); T. A. Alvesalo, T. Haavasoja, M. T. Manninen, and A. T. Soinne, Phys. Rev. Lett. 44, 1076 (1980).

[2]E. K. Zeise, Ph.D. thesis, Cornell University, 1981 (unpublished); E. K. Zeise, J. Saunders, A. I. Ahonen, C. N. Archie, and R. C. Richardson, Physica (Utrecht) 108B, 1213 (1981).

[3]W. P. Halperin, F. B. Rasmussen, C. N. Archie, and R. C. Richardson, J. Low Temp. Phys. 31, 617 (1978).

[4]A. C. Anderson, W. Reese, and J. C. Wheatley, Phys. Rev. 130, 495 (1963).

[5]W. R. Abel, A. C. Anderson, W. C. Black, and J. C. Wheatley, Phys. Rev. 147, 111 (1966).

[6]A. C. Mota, R. P. Platzeck, R. Rapp, and J. C. Wheatley, Phys. Rev. 177, 266 (1969).

[7]B. Hebral, G. Frossati, H. Godfrin, and D. Thoulouse, Phys. Lett. 85A, 290 (1981).

[8]D. F. Brewer, J. G. Daunt, and A. K. Sreedhar, Phys. Rev. 115, 836 (1959).

[9]M. Strongin, G. O. Zimmerman, and H. A. Fairbank, Phys. Rev. 128, 1983 (1962).

[10]B. M. Abraham, M. Durieux, C. J. van den Meijdenberg and D. W. Osborne, in *Low Temperature Physics—LT9, Proceedings of the Ninth International Conference on Low Temperature Physics, Ohio State University, Columbis, Ohio,* edited by J. G. Daunt (Plenum, New York, 1965).

[11]T. R. Roberts and S. G. Sydoriak, Phys. Rev. 98, 1672 (1955).

[12]B. M. Abraham, D. W. Osborne, and B. Weinstock, Phys. Rev. 98, 551 (1955).

[13]D. S. Greywall and P. A. Busch, Phys. Rev. Lett. 49, 146 (1982).

[14]Emerson and Cuming, Canton, Mass., Type 1266.

[15]Leico Industries, Inc., New York.

[16]K. Andres and W. O. Sprenger, in *Proceedings of the 14th International Conference on Low Temperature Physics,* edited by M. Krusuis and M. Vuorio (North-Holland, Amsterdam, 1975), Vol. 1, p. 123.

[17]D. S. Greywall, Phys. Rev. B 18, 2127 (1978).

[18]G. J. Sellers and A. C. Anderson, Rev. Sci. Instrum. 45, 1256 (1974).

[19]J. C. Ho and N. E. Phillips, Rev. Sci. Instrum. 36, 1382 (1965).

[20]P. R. Roach, J. B. Ketterson, and M. Kuchnir, Rev. Sci. Instrum. 43, 898 (1972).

[21]D. S. Greywall and P. A. Busch, J. Low Temp. Phys. 46, 451 (1982).

[22]D. S. Greywall and P. A. Busch, Rev. Sci. Instrum. 51, 509 (1980).

[23]Metrologia 15, 65 (1979).

[24]D. S. Greywall, Phys. Rev. B 23, 2152 (1981).

[25]E. Ihota, M. T. Manninen, J. P. Pekola, A. T. Soinne, and R. J. Soulen, Phys. Rev. Lett. 47, 590 (1981).

[26]R. J. Soulen, H. Marshak, and J. H. Colwell, private communication.

[27]E. C. Kerr and R. D. Taylor, Ann. Phys. (N.Y.) 20, 450 (1962).

[28]E. R. Grilly, J. Low Temp. Phys. 4, 615 (1971).

[29]E. R. Grilly and E. F. Hammel, in *Progress in Low Temperature Physics,* edited by C. J. Gorter (North-Holland, Amsterdam, 1961), Vol. 3, see footnote on p. 122.

[30]R. H. Sherman and F. J. Edeskuty, Ann. Phys. (N.Y.) 9, 522 (1960).

[31]C. Boghosian, H. Meyer, and J. E. Rives, Phys. Rev. 146, 110 (1966).

[32]B. M. Abraham and D. W. Osborne, J. Low Temp. Phys. 5, 355 (1971).

[33]D. F. Brewer and J. G. Daunt, Phys. Rev. 115, 843 (1959).

[34]D. S. Greywall, Phys. Rev. B 15, 2604 (1977).

[35]B. M. Abraham (unpublished).

[36]B. Weinstock, B. M. Abraham, and D. W. Osborne, Nuovo Cimento 9, 310 (1958).

[37]P. R. Roach, M. W. Meisel, and Y. Eckstein, Phys. Rev. Lett. 48, 330 (1982).

[38]S. Doniach and S. Engelsberg, Phys. Rev. Lett. 17, 750 (1966).

[39]N. F. Berk and J. R. Schrieffer, Phys. Rev. Lett. 17, 433 (1966).

[40]C. J. Pethick and G. M. Carneiro, Phys. Rev. A 7, 304 (1973).

[41]G. Baym and C. J. Pethick, in *The Physics of Liquid and Solid Helium,* edited by K. H. Bennemann and J. B. Ketterson (Wiley, New York, 1978), Part II.

[42]W. F. Brinkman and S. Engelsberg, Phys. Rev. 169, 417 (1968).

[43]J. C. Wheatley, Rev. Mod. Phys. 47, 415 (1975).

[44]C. J. Pethick, H. Smith, and P. Bhattacharyya, Phys. Rev. B 15, 3384 (1977).

[45]W. R. Abel, R. T. Johnson, J. C. Wheatley, and W. Zimmermann, Jr., Phys. Rev. Lett. 18, 737 (1967).

[46]D. D. Osheroff, W. van Roosbroeck, H. Smith, and W. F. Brinkman, Phys. Rev. Lett. 38, 134 (1977).

[47]G. E. Brown, C. J. Pethick, and A. Zaringhalam, J. Low Temp. Phys. 48, 349 (1982).

[48]S. Fantoni, V. R. Pandharipande, and K. E. Schmidt, Phys. Rev. Lett. 48, 878 (1982).